

Photon absorption edge in superconductors and gapped one-dimensional systems

V. V. Mkhitarian,¹ E. G. Mishchenko,¹ M. E. Raikh,¹ and L. I. Glazman²

¹*Department of Physics, University of Utah, Salt Lake City, Utah 84112, USA*

²*Department of Physics, Yale University, New Haven, Connecticut 06520, USA*

(Received 9 September 2009; published 18 November 2009)

Opening of a gap in the low-energy excitations spectrum affects the power-law singularity in the photon absorption spectrum $A(\Omega)$. In the normal state, the singularity, $A(\Omega) \propto [D/(\Omega - \Omega_{\text{th}})]^\alpha$, is characterized by an interaction-dependent exponent α . On the contrary, in the superconducting state the divergence, $A(\Omega) \propto (D/\Delta)^\alpha (\Omega - \tilde{\Omega}_{\text{th}})^{-1/2}$, is interaction independent, while threshold is shifted, $\tilde{\Omega}_{\text{th}} = \Omega_{\text{th}} + \Delta$; the “normal-metal” form of $A(\Omega)$ resumes at $(\Omega - \tilde{\Omega}_{\text{th}}) \geq \Delta \exp(1/\alpha)$. If the core hole is magnetic, it creates in-gap states; these states transform drastically the absorption edge. In addition, processes of scattering off the magnetic core hole involving spin-flip give rise to inelastic absorption with one or several *real* excited pairs in the final state, yielding a structure of peaks in $A(\Omega)$ at multiples of 2Δ above the threshold frequency. The above conclusions apply to a broad class of systems, e.g., Mott insulators, where a gap opens at the Fermi level due to the interactions.

DOI: [10.1103/PhysRevB.80.205416](https://doi.org/10.1103/PhysRevB.80.205416)

PACS number(s): 74.25.Gz, 74.50.+r, 73.40.Gk

I. INTRODUCTION

It was demonstrated more than 40 years ago¹⁻³ that electron x-ray absorption coefficient in metal, $A(\omega)$, is strongly modified by attraction to the localized hole left behind. The threshold behavior of absorption coefficient was found to be

$$A(\omega) = \mathcal{A}_0 \left(\frac{D}{\omega} \right)^\alpha. \quad (1)$$

In Eq. (1) and thereafter, $\omega = \Omega - \Omega_{\text{th}}$ stands for the difference between the photon energy and the core-hole energy measured from the Fermi level, and D is the bandwidth. Prefactor, \mathcal{A}_0 , contains the square of the dipole matrix element between the level and the conduction band. In the simplest case of a weak short-range attraction, $V(\mathbf{r}) < 0$, of electron to the hole the expression for the exponent $\alpha \ll 1$ has a form

$$\alpha = 2\nu_0 \left| \int d\mathbf{r} V(\mathbf{r}) \right|, \quad (2)$$

where ν_0 is the density of states at the Fermi level (we neglect the correction, $-\alpha^2/4$, originating from the Anderson orthogonality catastrophe²). Since the diverging absorption Eq. (1) comes from all energy scales between ω and D , it is quite robust. In a finite system, the threshold behavior depends on additional energy scale, the level spacing.⁴

Interest to the singular behavior of $A(\omega)$ near the threshold got a boost after it was predicted⁵ that this behavior manifests itself in the resonant-tunneling current-voltage characteristics. This prediction was later confirmed in numerous experiments.⁶⁻¹² Enhancement of absorption Eq. (1) was derived under the assumption that the density of states, $\nu(\omega)$, is constant $\nu(\omega) = \nu_0$ within the entire frequency interval, $(-D, D)$. If there is a gap, 2Δ , at the Fermi level the threshold behavior of $A(\omega)$ is singular even without interaction with a hole:

$$A(\omega) \propto \nu(\omega) = \nu_0 \frac{\omega}{(\omega^2 - \Delta^2)^{1/2}}, \quad (3)$$

and diverges near the edge of the gap. For small α it could be expected¹³ that this strong bare singularity is weakly affected by the excitonic effects.¹ Indeed, the low energy, $< 2\Delta$, many-body processes across the gap, responsible for Mahan singularity, are suppressed. This reasoning suggests the form of the absorption in superconductor

$$A(\omega) = \mathcal{A}_0 \left(\frac{D}{\Delta} \right)^\alpha \frac{\nu(\omega)}{\nu_0}. \quad (4)$$

Equation (4) crosses over to the conventional behavior Eq. (1) at high frequencies, ω , such that $\alpha \ln(\omega/\Delta) \sim 1$; in this frequency domain the effect of superconductivity is negligible, since $\omega \gg \Delta$.

Even stronger modification of the absorption spectrum takes place, when the core hole possesses a spin, so that the interaction with excited electron includes exchange. In this case, two physical mechanisms come into play. First, a core hole creates in-gap states¹⁴ with binding energy $\varepsilon_0 \sim \alpha^2 \Delta$ measured from the edges. These states, in turn, affect dramatically the elastic scattering of excited electron transforming the near-gap absorption into

$$A(\omega) = \frac{\mathcal{A}_0}{\sqrt{2}} \left(\frac{D}{\Delta} \right)^\alpha \frac{[\Delta(\omega - \Delta)]^{1/2}}{(\omega - \Delta) + \varepsilon_0}, \quad (5)$$

see Fig. 1. The absorption is zero at the threshold and resumes $(\omega - \Delta)^{-1/2}$ falloff only for $(\omega - \Delta) \gg \varepsilon_0$. As a “compensation” of the suppressed absorption, a δ -peak

$$A(\omega) = \frac{\mathcal{A}_0}{\sqrt{2}} \left(\frac{D}{\Delta} \right)^\alpha \sqrt{\Delta \varepsilon_0} \delta(\omega - \Delta + \varepsilon_0), \quad (6)$$

emerges at the position of the bound state.

There is another many-body feature in $A(\omega)$, which is specific for the exchange interaction with core hole. This feature originates from the fact that exchange interaction of

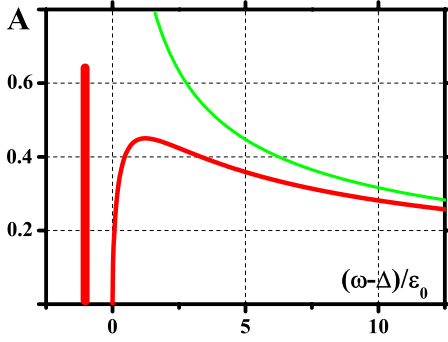


FIG. 1. (Color online) Absorption spectrum near the threshold for spinless [green (gray)] and spinful [red (black)] core hole.

electron with localized magnetic impurity in metal can be accompanied by creation of an electron-hole pair.¹⁵ The underlying reason is that localized spin emerges as a result of the on-site Hubbard repulsion of two electrons. On the other hand, with electron-electron interaction, *two electrons* can be excited by a *single photon*.^{16,17} In the presence of a rigid superconducting gap, this process starts from the threshold¹⁸ $\omega = \omega_1 = 3\Delta$, which corresponds to *inelastic* absorption with electron and additional pair in the final state. This process is schematically illustrated in Fig. 2(b). More additional pairs in the final state give rise to anomalies at $\omega = \omega_n = (2n+1)\Delta$, which have the form

$$\frac{\delta A(\omega)}{A(n\Delta)} \sim \alpha^{2n} (\omega - \omega_n)^{n-1/2} \theta(\omega - \omega_n). \quad (7)$$

II. DERIVATION OF EQ. (4)

A. Time dependent superconducting Green functions

An efficient way² to derive Eq. (1) is to consider scattering of excited electron by a transient potential, $V(\mathbf{r})\theta(t)$, and

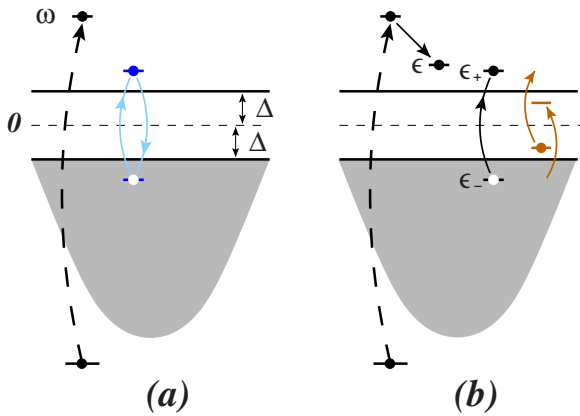


FIG. 2. (Color online) (a) Schematic illustration of elastic absorption, and (b) inelastic absorption. Blue (gray) lines illustrate creation and annihilation of a *virtual* pair that participates in *elastic* absorption. Final state of inelastic absorption is electron with energy ϵ and a *real* pair, (ϵ_+, ϵ_-) . Brown lines in (b) (thin arrowed lines on the right): since inelastic absorption is possible *only* for a spinful core hole, in-gap states created by this hole (Ref. 14) can also participate in absorption.

perform calculation in the time representation. In this representation, the Green function of the normal metal $G_0(t) = \int d\omega e^{i\omega t} \sum_q 1/(\omega - \xi_q \pm i0)$ (+ or - depending on $\text{sgn}(\xi_q)$) has the form $G_0(t) = -\nu_0 [t - iD^{-1} \text{sgn}(t)]^{-1}$, where D is the bandwidth. Generalization of the scattering approach to superconductor requires the time representation of the superconducting single-particle Green function

$$\hat{G}(\omega, q) = \frac{\hat{\Lambda}_+(q)}{\omega - \epsilon_q + i0} + \frac{\hat{\Lambda}_-(q)}{\omega + \epsilon_q - i0}, \quad (8)$$

where $\epsilon_q = \sqrt{\xi_q^2 + \Delta^2}$ is the spectrum of superconductor; $\xi_q = v_F q$ with $q = (k - k_F)$ being the momentum measured from the Fermi momentum, k_F , and v_F is the Fermi velocity. The projection operators $\hat{\Lambda}_\pm(q)$ are 2×2 matrices

$$\hat{\Lambda}_\pm(q) = \frac{1}{2} \begin{pmatrix} 1 \pm \frac{\xi_q}{\sqrt{\xi_q^2 + \Delta^2}} & \mp \frac{\Delta}{\sqrt{\xi_q^2 + \Delta^2}} \\ \mp \frac{\Delta}{\sqrt{\xi_q^2 + \Delta^2}} & 1 \pm \frac{\xi_q}{\sqrt{\xi_q^2 + \Delta^2}} \end{pmatrix}, \quad (9)$$

with following properties: $\hat{\Lambda}_\pm^2(q) = \hat{\Lambda}_\pm(q)$ and $\hat{\Lambda}_+(q) + \hat{\Lambda}_-(q) = 1$. In the basis of eigenfunctions of the Bogoliubov-de Gennes Hamiltonian, interaction with the short-range potential is described by the diagonal matrix

$$V_q = -\frac{\alpha}{2\nu_0} \hat{V}; \quad \hat{V} = \begin{pmatrix} 1 & 0 \\ 0 & -1 \end{pmatrix}. \quad (10)$$

Note that time-dependent 2×2 Green function of a superconductor, obtained as a result of integration $d\omega e^{i\omega t}$ of Eq. (8), and subsequent summation over momentum, q , can be conveniently expressed in terms of zeroth and first-order Bessel functions, namely

$$\hat{G}(t) = \begin{pmatrix} G(t) & F(t) \\ F(t) & G(t) \end{pmatrix}, \quad (11)$$

where the normal and anomalous Green functions, $G(t)$ and $F(t)$, are given by

$$G(t)|_{D>1} = \frac{\pi\Delta\nu_0}{2} \text{sgn}(t) [iJ_1(\Delta|t|) + Y_1(\Delta|t|)], \quad (12)$$

$$F(t)|_{D>1} = -i \frac{\pi\Delta\nu_0}{2} [iJ_0(\Delta|t|) + Y_0(\Delta|t|)]. \quad (13)$$

In the limit $\Delta \rightarrow 0$ the normal-metal Green function, $G_0(t)$, is recovered from Eq. (12) by using the small- t asymptote $Y_1(\Delta t) \approx -2/(\pi\Delta t)$, while $F(t) \rightarrow 0$.

B. Shape of the absorption edge

In superconductor, we generalize the response function to a 2×2 matrix, $\hat{L}(t)$, so that the absorption coefficient is given by the diagonal matrix element

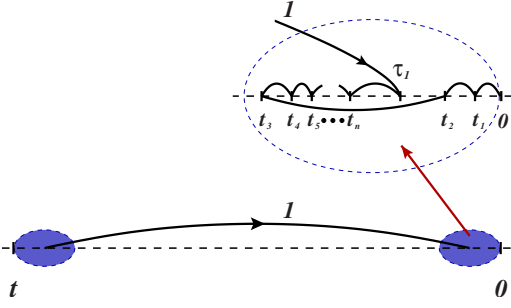


FIG. 3. (Color online) Conventional arrangement of times (Ref. 2) in n -fold integral Eq. (16) describing contribution to the response function due to n successive scatterings by the core hole. Time intervals, $|t_i - t_{i+1}|$, are distributed unevenly; central interval corresponding to line 1 is only slightly smaller than $|t|$. Remaining intervals contained in the boundary ellipses are $\ll |t|$. Inset: blowup of the right end of the line 1.

$$A(\omega) = \frac{A_0}{\pi\nu_0} \text{Re} \int_{-\infty}^0 dt \exp(-i\omega t) [\hat{L}(t)]_{11}. \quad (14)$$

As a result of matrix generalization, the expansion of the response function in powers of α ,

$$\hat{L}(t) = \sum_n \left(-\frac{\alpha}{2\nu_0} \right)^n \hat{L}_n(t), \quad (15)$$

has the 2×2 coefficients, $\hat{L}_n(t)$, which are given by the following n -fold integrals^{2,5} of the single-particle Green function, $\hat{G}(t)$,

$$\hat{L}_n(t) = i \int_t^0 dt_1 \cdots \int_t^0 dt_n \hat{G}(-t_1) \hat{V} \hat{G}(t_1 - t_2) \hat{V} \cdots \hat{V} \hat{G}(t_n - t). \quad (16)$$

In the normal metal, evaluation of $A(\omega)$ is based on exact analytical result² for the infinite sum

$$\begin{aligned} & \sum_{n=0}^{\infty} \left(-\frac{\alpha}{2\nu_0} \right)^n \int_t^0 dt_1 \cdots \int_t^0 dt_n G_0(\tau - t_1) \cdots G_0(t_n - \tau') \\ & = G_0(\tau - \tau') \left[\frac{(t - \tau)\tau'}{(t - \tau' + iD^{-1})(\tau + iD^{-1})} \right]^{\alpha/2}. \end{aligned} \quad (17)$$

To arrive to Eq. (1) one has to set $\tau=0$ and $\tau'=t$, after which the square bracket in Eq. (17) reduces to $(-iD)^{\alpha}$, and integrate $dt \exp(-i\omega t)$. Characteristic times t_i in the relation Eq. (17) are arranged unevenly as illustrated in Fig. 3. The central interval is $\approx t$, so that t_i are located in the close proximity, τ_1 or τ_2 (see Fig. 3) either to 0 or to t . It is important that in superconducting case the arrangement remains the same, and moreover, as we will see, $\Delta\tau_1$ and $\Delta\tau_2$ are always $\ll 1$. This means that $\hat{G}(t_i - t_{i+1})$ can be replaced by $G_0(t_i - t_{i+1})$ times the unit matrix. As a result, the matrix structure of \hat{V} drops out. The only Green function that retains the matrix structure is $\hat{G}(\tau_1 + \tau_2 - t)$, Fig. 3. However, in the component \hat{L}_{11} , the anomalous Green function drops out, so that

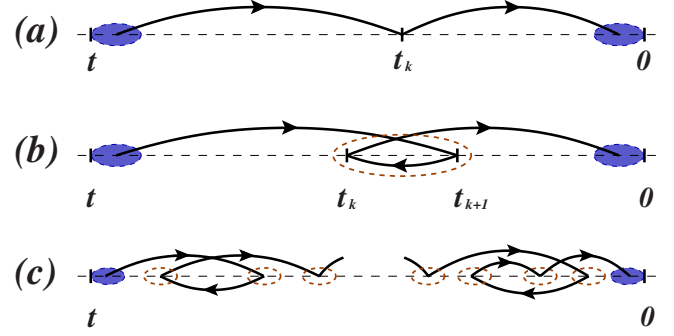


FIG. 4. (Color online) Examples of “unconventional” time domains in the integrand of Eq. (16): (a): Position of the point, t_1 , such that $|t_1| \gg \Delta^{-1}$, $|t - t_1| \gg \Delta^{-1}$, does not contribute to \hat{L}_n by virtue of Eq. (22); (b): As long as $|t_1| \gg \Delta^{-1}$, $|t - t_1| \gg \Delta^{-1}$, and $|t_2| \gg \Delta^{-1}$, $|t - t_2| \gg \Delta^{-1}$, contribution of the arrangement of times vanishes upon integration over t_1 or t_2 , see Eq. (26); (c): For the same reason, “long” ($\gg \Delta^{-1}$) intervals in the general “unconventional” arrangement yield vanishing contribution to \hat{L}_n , and thus, to the absorption at the threshold, $(\omega - \Delta) \ll \Delta$.

$$\hat{L}_{11}(t) \approx i(iD)^{\alpha} \alpha^2 \int_0^{|t|} \frac{d\tau_1 d\tau_2}{(\tau_1 \tau_2)^{1-\alpha/2}} G(-\tau_1 - \tau_2 - t), \quad (18)$$

$\tau_1 + \tau_2 \leq |t|$

where $G(t)$ is defined by Eq. (12). Equation (4) immediately follows from Eqs. (18) and Eq. (14). The Green’s function G in Eq. (18) generates the density of states, $\nu(\omega)$, in Eq. (4). One point should be clarified with regard to the validity of the above result Eq. (18). We used the normal-metal solution Eq. (17). This is justified since integrals over τ_1, τ_2 in Eq. (18) come from $\tau_1, \tau_2 \sim \Delta^{-1} \exp(-1/\alpha)$. This also validates the assumption $\Delta\tau_1, \Delta\tau_2 \ll 1$, which we used to disregard the matrix structure of $\hat{G}(t_i - t_{i+1})$.

C. Unconventional arrangements of times

There still remains a question whether or not the matrix structure of the superconducting Green functions, which becomes important near the threshold $(\omega - \Delta) \ll \Delta$, gives rise to the contributions to $A(\omega)$, caused by “unconventional” arrangements of times, t_i , ($|t_i| \gg \Delta^{-1}$), as shown in Figs. 4(a) and 4(b); these arrangements are not relevant in the normal-metal case. For example, the simplest such “unconventional” arrangement, Fig. 4(a), manifests itself as an extra combination

$$\int_t^0 dt_k \hat{G}(t_{k-1} - t_k) \hat{V} \hat{G}(t_k - t_{k+1}) \quad (19)$$

in the integrand Eq. (16). Since the arguments of \hat{G} in Eq. (19) are large, one can use the long-time asymptote

$$\hat{G}(t)|_{|t| \gg 1} \approx G_S(t) \begin{pmatrix} 1 & -\text{sgn}(t) \\ -\text{sgn}(t) & 1 \end{pmatrix}, \quad (20)$$

where the $G_S(t)$ is the $\Delta t \gg 1$ asymptote of Eq. (12)

$$G_S(t) = \nu_0 \operatorname{sgn}(t) \left(\frac{\pi\Delta}{2|t|} \right)^{1/2} i e^{-i\Delta|t|+3\pi/4}. \quad (21)$$

Note however, that the matrix structure in the integrand of Eq. (19) is

$$\begin{pmatrix} 1 & -1 \\ -1 & 1 \end{pmatrix} \begin{pmatrix} 1 & 0 \\ 0 & -1 \end{pmatrix} \begin{pmatrix} 1 & -1 \\ -1 & 1 \end{pmatrix} = 0. \quad (22)$$

Thus, we turn to the next possible arrangement of times Fig. 4(b); the corresponding combination in Eq. (16) coming from this arrangement reads

$$\int_t^0 dt_k \int_t^0 dt_{k+1} \hat{G}(t_{k-1}-t_k) \hat{V} \hat{G}(t_k-t_{k+1}) \hat{V} \hat{G}(t_{k+1}-t_{k+2}). \quad (23)$$

To integrate over t_k , we perform multiplication of the first three matrices and obtain

$$\begin{aligned} G_S(t_{k-1}-t_k) & \begin{pmatrix} 1 & -1 \\ -1 & 1 \end{pmatrix} \begin{pmatrix} 1 & 0 \\ 0 & -1 \end{pmatrix} \begin{pmatrix} G(t_k-t_{k+1}) & F(t_k-t_{k+1}) \\ F(t_k-t_{k+1}) & G(t_k-t_{k+1}) \end{pmatrix} \\ & = G_S(t_{k-1}-t_k) [G(t_k-t_{k+1}) + F(t_k-t_{k+1})] \begin{pmatrix} 1 & 1 \\ -1 & -1 \end{pmatrix}. \end{aligned} \quad (24)$$

Then the integration over t_k in Eq. (23) reduces to

$$\int_{t_{k+2}-t_{k+1}}^{t_{k-1}-t_{k+1}} d\tau [G(\tau) + F(\tau)] G_S(t_{k-1}-t_{k+1}-\tau), \quad (25)$$

where we introduced a variable $\tau = t_k - t_{k+1}$. Typical distance between the points, $|t_{k-1} - t_{k+1}|$ and $|t_{k+1} - t_{k+2}|$, is $\gg \Delta^{-1}$, which suggests that the limits of integration can be extended to $\pm\infty$. Upon this extension we get

$$\frac{e^{i\Delta(t_{k+1}-t_{k-1})}}{\sqrt{|t_{k+1}-t_{k-1}|}} \int_{-\infty}^{\infty} d\tau [G(\tau) + F(\tau)] e^{i\Delta\tau}, \quad (26)$$

which is identical zero. The same reasoning rules out¹⁹ the more complex “unconventional” arrangements of times *at the threshold*, such as the ones shown in Fig. 4(c). These arrangements, however, become essential in the case of exchange interaction with core hole, to which we now turn.

III. EXCHANGE INTERACTION WITH CORE HOLE

Exchange interaction with core hole corresponds to replacement

$$V(\mathbf{r}) \rightarrow J\delta(\mathbf{r})(\mathbf{S} \cdot \boldsymbol{\sigma}), \quad (27)$$

where \mathbf{S} is a localized spin, and $\boldsymbol{\sigma}$ is electron spin operator. To illustrate the dramatic impact which the exchange interaction has on the near-threshold absorption, we return to Fig. 4(a) and corresponding expression Eq. (19). For potential interaction with core hole, this expression was identical zero by virtue of relation Eq. (22). Recall now that in the stationary problem the diagonal part of the exchange interaction,

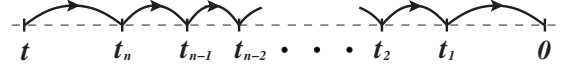


FIG. 5. For exchange interaction with the core hole, “unconventional” arrangement of times, $(t_i - t_{i+1}) \gg \Delta^{-1}$, dominates the near-threshold, $(\omega - \Delta) \ll \Delta$ absorption. Odd n describes the absorption peak at $\omega = \Delta - \varepsilon_0$.

$V(\mathbf{r})S^z\sigma^z$, creates two in-gap bound states:¹⁴ one below the upper edge by

$$\varepsilon_0 = \frac{\pi^2 \alpha^2 \Delta}{8}, \quad (28)$$

and one above the lower edge by ε_0 . The reason behind this effect is that $S^z\sigma^z$ effectively transforms the operator \hat{V} in Eq. (10) into the unity matrix. An immediate consequence of this transformation for our calculation is that the contribution Eq. (19) becomes *finite*. Subsequently, the contribution Fig. 4(b) and all higher-order “unconventional” contributions illustrated in Fig. 5(a) are also finite. Within our formalism, the in-gap bound states emerge as poles, $1/[\omega \pm (\Delta - \varepsilon_0)]$, of the Green function upon summation²⁰ of infinite series of diagrams.

In deriving Eq. (5) for $A(\omega)$ near the threshold, we in fact repeat all the steps which would render the stationary in-gap states. Namely, we notice that the phase $\Delta \sum_k |t_{k+1} - t_k|$ of the integrand in Eq. (16) is *large*, which insures that the dominant contribution to $L_n(t)$ comes from the domain $0 < t_1 < t_2 \cdots < t_n$, see Fig. 5(a), when the net phase is Δt ; contributions from the domains where t_m are not ordered are suppressed by oscillations of the integrand. Thus we conclude that the integral Eq. (16) is dominated by $t_m \sim t(m/n)$. For the asymptote Eq. (21) to be applicable in this domain, the condition $(t_{m+1} - t_m) \sim t/n \gg \Delta^{-1}$ must be met. With t_m ordered, the n -fold integration in Eq. (16) can be carried out with the help of the identity

$$\int_a^b \frac{dx}{\sqrt{(x-a)(b-x)}} = \pi. \quad (29)$$

Depending on the parity of n , the remaining integration, upon introducing the variables $z_i = t_i/t$, reduces to

$$\int_0^1 dz_1 \int_{z_1}^1 dz_2 \cdots \int_{z_{(n-3)/2}}^1 dz_{(n-1)/2} = \frac{1}{\Gamma\left(\frac{n+1}{2}\right)} \quad (30)$$

for odd n , or to

$$\int_0^1 dz_1 \int_{z_1}^1 dz_2 \cdots \int_{z_{n/2-1}}^1 dz_{n/2} (1 - z_{n/2})^{-1/2} = \frac{\sqrt{\pi}}{\Gamma\left(\frac{n+1}{2}\right)} \quad (31)$$

for even n . Finally we get

$$[\hat{L}_n(t)]_{11} = (-1)^n \left(\frac{\pi^2 \nu_0^2 \Delta}{2} \right)^{n+1/2} \frac{(-it)^{n-1/2}}{\Gamma\left(\frac{n+1}{2}\right)} e^{i\Delta t}. \quad (32)$$

The product, $\alpha^n \hat{L}_n(t)$, has a sharp maximum at $n \sim \alpha^2 \Delta t$, so that $\Delta t/n \sim 1/\alpha^2$ is large, which justifies the above assumption ($t_{m+1} - t_m \gg \Delta^{-1}$).

The sum over even n , $\hat{L}_{\text{even}}(t) = \sum_{\text{even}} (\alpha/2\nu_0)^n \hat{L}_n(t)$, leads to the result Eq. (5). Most conveniently it can be seen by transforming to the frequency domain, since the expansion of Eq. (5) in powers of α^2 has a form

$$A(\omega) = \mathcal{A}_0 \left(\frac{\Delta}{2} \right)^{1/2} \sum_{p=0}^{\infty} \left(\frac{\pi^2 \alpha^2 \Delta}{8} \right)^p \frac{(-1)^p}{(\omega - \Delta)^{p+1/2}}. \quad (33)$$

This expansion coincides term by term with the sum,

$$\mathcal{A}_0 \sum_p \left(-\frac{\alpha}{2\nu_0} \right)^{2p} \int_{-\infty}^0 dt [\hat{L}_{2p}(t)]_{11} \exp(-i\omega t), \quad (34)$$

with $\hat{L}_{2p}(t)$ given by Eq. (32). The sum over odd terms results in a simple exponent,

$$\hat{L}_{\text{odd}}(t) = \sum_{\text{odd}} \left(-\frac{\alpha}{2\nu_0} \right)^n \hat{L}_n(t) \propto \exp[i(\Delta - \varepsilon_0)t]. \quad (35)$$

This exponent gives rise to the δ -peak, Eq. (6), in the absorption spectrum.

IV. INELASTIC ABSORPTION

Up to now we neglected the spin-flip part,

$$J\delta(\mathbf{r})[S^+ \sigma^- + S^- \sigma^+], \quad (36)$$

of the exchange interaction. As it was mentioned in the Introduction, this spin-flip part of interaction between electron and core hole creates an effective electron-electron scattering.¹⁵ This explains the possibility of inelastic processes with three quasiparticles in the final state, as illustrated in Fig. 2(b). The threshold of inelastic process is $\omega = 3\Delta$. Here, we will restrict ourselves only to the behavior of inelastic absorption away from the threshold, $(\omega - 3\Delta) \gg \varepsilon_0$, and follow the calculation in Ref. 18. A great simplification away from threshold is that a “golden-rule”-based calculation is sufficient. The rate of the process depicted in Fig. 2(b) is given by the following sum over the quasiparticle states with energies, ε , ε_+ , and ε_- ,

$$W(\omega) = 2\pi \sum_{\varepsilon, \varepsilon_+, \varepsilon_-} \left| \frac{\alpha_{sf}}{\omega - \varepsilon} \right|^2 \delta(\omega - \varepsilon - \varepsilon_+ + \varepsilon_-), \quad (37)$$

where the first factor is the square of the amplitude, which is nonzero since the process involves a spin-flip,¹⁵ and the dimensionless spin-flip coupling constant is

$$\alpha_{sf} = J\nu_0 \sqrt{S(S+1)}. \quad (38)$$

Near the threshold, $\omega = 3\Delta$, we have $\varepsilon \approx \Delta$, $\varepsilon_+ \approx \Delta$, and $\varepsilon_- \approx -\Delta$. The matrix element near the threshold is approximately constant. This simplifies the summation in Eq. (37) to

$$\begin{aligned} W(\omega) &= \frac{\pi \alpha_{sf}^2}{2\Delta^2} \\ &\times \int_{\Delta}^{\infty} d\varepsilon \nu(\varepsilon) \int_{\Delta}^{\infty} d\varepsilon_+ \nu(\varepsilon_+) \int_{-\infty}^{-\Delta} d\varepsilon_- \nu(\varepsilon_-) \delta(\omega - \varepsilon - \varepsilon_+ + \varepsilon_-), \\ &= \frac{\pi^2 \alpha_{sf}^2}{2} \left(\frac{\omega - 3\Delta}{2\Delta} \right)^{1/2}. \end{aligned} \quad (39)$$

Note that in the close vicinity of the threshold, $|\omega - 3\Delta| \lesssim \varepsilon_0$, in-gap states created by the spinful core hole participate in the absorption, as illustrated in Fig. 2(b). Namely, a pair of quasiparticles in the final state can consist, e.g., of one quasiparticle excited above the gap and empty lower in-gap state.

V. DISCUSSION

Our results Eqs. (4) and (5) establish the threshold behavior of $A(\omega)$ for a general situation when the density of states is strongly modified near the Fermi level but assumes a constant value away from the Fermi level. A notable example is a one-dimensional (1D) *interacting* system. The shape of the Fermi-edge singularity in 1D interacting electron gas in the Luttinger-liquid regime has been studied in²¹ using the bosonization technique. Backscattering plays an important role in the exponent of the absorption. When backscattering opens a gap, the physics described in the present paper comes into play. The case of 1D Mott insulator near half filling makes the behavior of $A(\omega)$ even richer, since the doping shifts the threshold. A related example is the Peierls insulator, when the charge density wave and ensuing gap at the Fermi level are due to electron-phonon interactions. Note, that in the latter case the gap is orders of magnitude larger than in superconductor.

Speaking about conventional setting for Fermi-edge absorption in metals, singularity in $A(\omega)$ is smeared due to the finite lifetime, γ , of the core hole. In our consideration we assumed that the gap, 2Δ , exceeds γ . In most experiments in metals the smearing of the edge is a fraction of eV, i.e., much bigger than a typical 2Δ -value. However, the origin of this smearing is not a natural core hole lifetime broadening but rather a finite instrumental resolution.²² The fact that observed absorption shape is a convolution of the singular $A(\omega)$, a Gaussian, which is measurement-related, and a Lorentzian, describing natural core hole lifetime, allows to separate the two contributions to the edge smearing. Early attempts²³ of such separation yielded $\gamma = 40$ meV for $2p$ core hole. In the other experiment²⁴ involving core hole four times shallower than in Ref. 23, the natural width was found to be four times smaller, $\gamma = 10$ meV. In later experiment,²⁵ where the full broadening, 29 meV, was very small, analysis of the data for the same absorption line as in Ref. 24 revealed even smaller value of the core hole width in simple metals, $\gamma = 4$ meV.

As a final remark, the relevance of the exchange interaction of electron with the core hole was first pointed out in Ref. 26.

ACKNOWLEDGMENTS

We acknowledge the hospitality of the KITP at UCSB, where research was supported in part by the National Science Foundation under Grant No. PHY05-51164. We also

acknowledge the support of DOE under Grant No. DE-FG02-06ER46313 (E.M.), Petroleum Research Fund under Grant No. 43966-AC10 (V.M. and M.R.), and NSF Grant No. under DMR-0906498 (L.G.).

-
- ¹G. D. Mahan, Phys. Rev. **163**, 612 (1967).
²P. Nozieres and C. T. De Dominicis, Phys. Rev. **178**, 1097 (1969).
³References to theoretical and experimental papers on the Fermi-edge singularity can be found in the review K. Ohtaka and Y. Tanabe, Rev. Mod. Phys. **62**, 929 (1990).
⁴M. Hentschel, D. Ullmo, and H. U. Baranger, Phys. Rev. B **76**, 245419 (2007).
⁵K. A. Matveev and A. I. Larkin, Phys. Rev. B **46**, 15337 (1992).
⁶A. K. Geim, P. C. Main, N. La Scala, L. Eaves, T. J. Foster, P. H. Beton, J. W. Sakai, F. W. Sheard, M. Henini, G. Hill, and M. A. Pate, Phys. Rev. Lett. **72**, 2061 (1994).
⁷E. E. Vdovin, Yu. N. Khanin, O. Makarovskiy, Yu. V. Dubrovskii, A. Patané, L. Eaves, M. Henini, C. J. Mellor, K. A. Benedict, and R. Airey, Phys. Rev. B **75**, 115315 (2007).
⁸D. H. Cobden and B. A. Muzykantskii, Phys. Rev. Lett. **75**, 4274 (1995).
⁹M. Gryglas, M. Baj, B. Chenaud, B. Jouault, A. Cavanna, and G. Faini, Phys. Rev. B **69**, 165302 (2004).
¹⁰H. Frahm, C. von Zobeltitz, N. Maire, and R. J. Haug, Phys. Rev. B **74**, 035329 (2006).
¹¹N. Maire, F. Hohls, T. Ludtke, K. Pierz, and R. J. Haug, Phys. Rev. B **75**, 233304 (2007).
¹²M. R uth, T. Slobodskyy, C. Gould, G. Schmidt, and L. W. Mollenkamp, Appl. Phys. Lett. **93**, 182104 (2008).
¹³Y. Ma, Phys. Rev. B **32**, 1472 (1985), to incorporate superconducting gap into $A(\omega)$, was restricted to the second order in α and yielded an unphysical result: finite in-gap absorption.
¹⁴A. I. Rusinov, JETP Lett. **9**, 85 (1969).
¹⁵A. Kaminski and L. I. Glazman, Phys. Rev. Lett. **86**, 2400 (2001).
¹⁶E. G. Mishchenko, M. Yu. Reizer, and L. I. Glazman, Phys. Rev. B **69**, 195302 (2004).
¹⁷J. Dai, M. E. Raikh, and T. V. Shahbazyan, Phys. Rev. Lett. **96**, 066803 (2006).
¹⁸V. V. Mkhitarian and M. E. Raikh, Phys. Rev. B **77**, 195329 (2008).
¹⁹It is easy to see that the singular contribution to $\hat{L}(t)$ emerges from the domain where t_{k+2}, t_{k+1} are close to t , while t_{k-1} is close to zero, see Fig. 4(b). In this domain, a large phase, $i3\Delta t$, is accumulated along the path, $0 \rightarrow t \rightarrow 0 \rightarrow t$. This phase readily transforms into anomalous contribution, $\propto \alpha^2 \sqrt{\omega - 3\Delta}$, to $A(\omega)$. On the other hand, it is apparent that this contribution, being *perturbative* in α , must be fictitious. Indeed, it can be demonstrated that this contribution is cancelled by the lowest-order shake-up process.
²⁰More precisely, to recover stationary in-gap states, one has to perform $(-\infty, \infty)$ integrations instead of limited integration intervals in Eqs. (14) and (16).
²¹A. O. Gogolin, Phys. Rev. Lett. **71**, 2995 (1993); C. L. Kane, K. A. Matveev, and L. I. Glazman, Phys. Rev. B **49**, 2253 (1994); G. A. Fiete, Phys. Rev. Lett. **97**, 256403 (2006).
²²P. H. Citrin, G. K. Wertheim, and M. Schl uter, Phys. Rev. B **20**, 3067 (1979).
²³P. H. Citrin, G. K. Wertheim, and Y. Baer, Phys. Rev. B **16**, 4256 (1977).
²⁴T. A. Callcott, E. T. Arakawa, and D. L. Ederer, Phys. Rev. B **18**, 6622 (1978).
²⁵P. A. Bruhwiler and S. E. Schnatterly, Phys. Rev. B **41**, 8013 (1990).
²⁶S. M. Girvin and J. J. Hopfield, Phys. Rev. Lett. **37**, 1091 (1976).